

LAKE WATER TEMPERATURE SIMULATION MODEL

By Midhat Hondzo¹ and Heinz G. Stefan,² Member, ASCE

ABSTRACT: Functional relationships to describe surface wind mixing, vertical turbulent diffusion, convective heat transfer, and radiation penetration based on data from lakes in Minnesota have been developed. These relationships have been introduced by regressing model parameters found either by analysis of field data or by calibration (minimizing the difference between measured and predicted temperatures) in simulations on individual lakes, against gross lake properties such as surface area or Secchi depth. Results of the deterministic lake water temperature stratification model using the functional relationships are not much different than results using the individual calibrations on a great variety of lake surface areas, depths, and transparencies. The model also requires no on-lake weather but uses input from existing off-lake weather stations. First order uncertainty analysis showed moderate sensitivity of simulated lake water temperatures to model coefficients. The numerical model which can be used without calibration has an average 1.1°C root mean square error, and 93% of measured lake water temperatures variability is explained by the numerical simulations, over wide ranges of lake morphometries, trophic levels, and meteorological conditions.

INTRODUCTION

Recent concern over climate change, acid rain pollution and other environmental problems has lead to renewed interest in numerical models that simulate the seasonal temperature cycle in lakes (McCormick 1990; Schertzer and Sawchuk 1990; Hondzo and Stefan 1991). To make water temperature projections for lakes of different geometries at different latitudes and altitudes, and to extrapolate to possible future climate scenarios, numerical simulation models are very useful if not indispensable.

Long-term behavior of lakes with different morphometries and trophic levels has become of interest. Water temperature data are often available for a few, possibly "nontypical" lakes in a region. To calibrate a lake water temperature model and to validate predictions on a regional scale can therefore be difficult. Some coefficients such as eddy diffusion coefficients or turbulence closure coefficients used in lake water temperature models are not universal due to their dependence on stratification, and the time scale of simulations as pointed out by Aldama et al. (1989). Meteorological data used as input to lake temperature simulation models are also not available at most lake sites but have to be taken from weather stations sometimes as much as 200 km away. This intraregional data transfer will contribute to prediction errors.

The purpose of this paper is to describe how the coefficients in a lake temperature model were generalized to fit a wide range of lake classes and meteorological conditions. To do this, new functional relationships had to be introduced for the calibration coefficients. The generalized model can

¹Res. Assoc., St. Anthony Falls Hydr. Lab., Dept. of Civ. and Min. Engrg., Univ. of Minnesota, Minneapolis, MN 55414.

²Prof. and Assoc. Dir., St. Anthony Falls Hydr. Lab., Dept. of Civ. and Min. Engrg., Univ. of Minnesota, Minneapolis, MN.

Note. Discussion open until April 1, 1994. To extend the closing date one month, a written request must be filed with the ASCE Manager of Journals. The manuscript for this paper was submitted for review and possible publication on May 26, 1992. This paper is part of the *Journal of Hydraulic Engineering*, Vol. 119, No. 11, November, 1993. ©ASCE, ISSN 0733-9429/93/0011-1251/\$1.00 + \$.15 per page. Paper No. 4125.

then be applied to lakes for which no site-specific calibration can be made, e.g., for a lack of data or lack of time. Fortunately, it can be demonstrated that the regional model makes predictions with almost the same order of accuracy as the model calibrated to particular lakes. Therefore, modeling regional and long-term lake temperature structure can be accomplished with the same confidence as modeling of short time behavior of particular lakes.

Lake temperature prediction models have been developed previously in various forms. Reviews have been presented by Harleman (1982), Henderson-Sellers and Davies (1989), and Imberger and Patterson (1989). A deterministic, process-oriented, unsteady, one-dimensional lake water quality model, which has been successfully applied over a period of years to simulate hydrothermal processes in individual lakes and for a variety of meteorological conditions (Stefan and Ford 1975; Stefan et al. 1980a; Ford and Stefan 1980) was used in this study. The model was previously expanded to include suspended sediment (Stefan et al. 1982), light attenuation (Stefan et al. 1983), phytoplankton growth, and nutrient dynamics (Riley and Stefan 1987). The hydrothermal part of the model was improved and generalized in this study as will be shown.

PREVIOUS TEMPERATURE PREDICTION MODEL

Model Formulation

In the model the lake is described by a system of horizontal layers, each of which is well mixed. Vertical transport of heat is described by a diffusion equation in which the vertical diffusion coefficient $K_z(z)$ is incorporated in a conservation equation of the form:

$$A \frac{\partial T}{\partial t} = \frac{\partial}{\partial z} \left(k_z A \frac{\partial T}{\partial z} \right) + \frac{H}{\rho_w c_p} \dots \dots \dots (1)$$

where $T(z, t)$ is water temperature as a function of depth (z) and time (t), $A(z)$ is the horizontal area of the lake as a function of depth, $H(z, t)$ is the internal distribution of heat sources due to radiation absorption inside the water column, ρ_w is the water density, and c_p is the specific heat of water.

The net heat input from the atmosphere is computed from a balance between incoming heat from solar and longwave radiation and the outflow of heat through convection, evaporation, and back radiation. The net increase in heat results in an increase in water temperature. The heat balance equation is given by

$$H_n = H_{sn} + H_{an} - H_c - H_e - H_{br} \dots \dots \dots (2)$$

where H_n = net heat input at the water surface ($\text{kcal m}^{-2}\text{day}^{-1}$), H_{sn} = net solar (short wave) radiation, H_{an} = net atmospheric long wave radiation, H_c = convective loss (sensible heat), H_e = evaporative loss (latent heat), and H_{br} = back radiation. The heat budget components in (2) are computed as follows:

$$H_{sn}(0) = (1 - r)\beta H_s \quad \text{at } z = 0 \dots \dots \dots (3a)$$

$$H_{sn} = (1 - r)(1 - \beta)H_s \quad \text{at } z > 0 \dots \dots \dots (3b)$$

where H_s = incoming solar radiation ($\text{kcal m}^{-2}\text{day}^{-1}$), r is the reflection coefficient computed as a function of the angle of incidence and the concentration of suspended sediment in the surface layer (Dhamotharan 1979;

Stefan et al. 1983). β = the surface absorption factor (Dake and Harleman 1969). The attenuation of solar radiation with depth follows Beer's law:

$$H_{sn}(i) = H_{sn}(i - 1)\exp(-\mu\Delta z) \quad (4)$$

where $H_{sn}(i - 1)$ = solar radiation at the top of a horizontal layer of water ($\text{kcal m}^{-2}\text{day}^{-1}$), $H_{sn}(i)$ = solar radiation at the bottom of a layer, Δz = thickness of a layer (m), and μ = the extinction coefficient (m^{-1})

$$\mu = \mu_w + \mu_{ss} \cdot SS + \mu_{chl} \text{Chla} \quad (5)$$

where μ_w = the extinction coefficient of lake water (m^{-1}), μ_{ss} = the specific extinction coefficient due to suspended sediment ($\text{l m}^{-1}\text{mg}^{-1}$); SS = suspended inorganic sediment concentration (mg l^{-1}); μ_{chl} = the extinction coefficient due to chlorophyll ($\text{m}^2\text{g}^{-1}\text{Chla}$) (Bannister 1974), Chla is chlorophyll-a concentration (g m^{-3}).

$$H_a = \sigma \varepsilon_a T_a^4 \quad (6)$$

where σ = Stefan-Boltzmann constant, T_a = absolute temperature ($^{\circ}\text{K}$), ε_a = atmospheric emissivity (Idso and Jackson 1969). Back radiation H_{br} follows the same formulation [(6)], but the emissivity is fixed at 0.975, and atmospheric temperature is replaced by water surface temperature T_s .

Aerodynamic bulk formulae were used to calculate surface wind shear τ , latent heat flux H_e , and the sensible heat flux H_c across the water surface:

$$\tau = \rho_a \overline{u'w'} = \rho_a u_*^2 = \rho_a C_d U_a^2 \quad (7)$$

$$H_c = \rho_a c_p \overline{\theta'w'} = \rho_a c_p C_s u_* \theta_* = \rho_a c_p f(U_a)(T_s - T_a) \quad (8)$$

$$H_e = \rho_a L_v \overline{q'w'} = \rho_a L_v C_l q_* u_* = \rho_a L_v f(U_a)(q_s - q_a) \quad (9)$$

where τ = the surface wind stress, ρ_a = the density of the air, u' and w' = turbulent fluctuations of velocity in horizontal and vertical direction; the overbar represents a time average; u_* = velocity scale, U_a = the wind speed above the water surface, C_d = the momentum or drag coefficient (Wu 1969), θ' = turbulent fluctuation in temperature, θ_* = temperature scale, C_s and C_l = heat transfer and vapor transfer coefficients respectively, and together with u_* are expressed as a function of wind speed, $f(U_a)$, (Ford 1976), T_s = water surface temperature, T_a = air temperature above the water surface, L_v = latent heat of vaporization, q' = the specific humidity fluctuation, q_* = the specific humidity scale, q_a = the specific humidity above the water surface, and q_s = the specific humidity at saturation pressure at the water surface temperature.

Turbulent kinetic energy (\overline{TKE}) supplied by wind shear and available for possible entrainment at the interface was estimated (Ford and Stefan 1980) by

$$TKE = W_{str} \int_{AS} U_* \tau dA \quad (10)$$

where A_s = lake surface area, U_* = shear velocity in the water, τ = shear stress at the air-water interface, and W_{str} = the wind sheltering coefficient.

The model distributes the surface heat input in the water column using turbulent diffusion (1) in response to wind and natural convection (Ford

and Stefan 1980). The numerical model is applied in daily time steps using mean daily values for the meteorological variables. Initial conditions, model setup parameters, and daily meteorological variables average air temperature (T_a), dew point temperature (T_d), wind speed (U_a), and solar radiation (H_s) have to be provided to use the model.

Model Coefficients

Model calibration coefficients needed for simulations of lake water temperatures are given in Table 1. These coefficients are kept at their initially specified value throughout the entire period of the simulation.

Maximum hypolimnetic eddy diffusivity is the threshold value for the turbulent diffusion under negligible stratification. In modeling this condition is assumed to be satisfied by small stability frequency, e.g., $N^2 = 7.5 \times 10^{-5} \text{ sec}^{-2}$. Maximum hypolimnetic eddy diffusivity range is from $8.64 \text{ m}^2 \text{ day}^{-1}$ for large lakes (Lewis 1983) to $0.086 \text{ m}^2 \text{ day}^{-1}$ for small lakes (Hondzo et al. 1991).

The wind sheltering coefficient (W_{str}) determines the fraction of turbulent kinetic energy from the wind applied at the lake surface and available for mixing. The coefficient can range from 0.1 to 1.0 depending on the size of the lake and the terrain surrounding the lake. The coefficient defines the "active" portion of the lake surface area on which wind shear contributes to the turbulent kinetic energy.

The wind function coefficient is defined for the neutral boundary layer above the lake surface. This condition occurs for the case of negligible atmospheric stratification. The wind speed function used is linear with the wind speed

$$f(U_a) = cU_a \dots\dots\dots (11)$$

where c is defined as a wind function coefficient and U_a is measured at 10 m above ground level at an off-lake site. The atmosphere above natural water bodies is often nearly neutrally stable. Thus a significant amount of experimental and theoretical work has been done in regard to wind function coefficient estimation [e.g., Dake (1972), Ford (1976), Stefan et al. (1980b), and Adams et al. (1990)]. Different ranges of coefficients were reported due to different measurement locations of the wind speed, U_a , in horizontal as well as vertical position relative to the lake surface. Herein the wind

TABLE 1. List of Calibration Coefficients with Ranges Used in Previous Simulations

Coefficient (1)	Symbol (2)	Units (3)	Range of Values	
			Previous simulations (4)	Literature values (5)
Radiation extinction by water	μ_w	(m^{-1})	0.4–0.65	0.02–2.0
Radiation extinction by chlorophyll	μ_{ch}	($\text{m}^2 \text{g}^{-1} \text{Chla}$)	8.65–16.0	0.2–31.4
Wind sheltering	W_{str}	(—)	0.1–0.9	0.1–1.0
Wind function coefficient	c	(—)	20.0–30.0	20.0–30.0
Maximum hypolimnetic eddy diffusivity	K_{zmax}	($\text{m}^2 \text{ day}^{-1}$)	0.1–2.0	0.086–8.64

function coefficient is taken to be in the range of 20–30 if wind speed is in mi h^{-1} , vapour pressure in mbar, and heat flux in $\text{kcal m}^{-2}\text{day}^{-1}$.

Radiation extinction coefficients by water (μ_w) and chlorophyll (μ_{ch}) specify the rate of attenuation of short-wave radiation energy as it penetrates through the water column. Both coefficients vary as a function of wavelength. Usually these coefficients are reported by a single mean spectral value for a given lake. Smith and Baker (1981) measured a range of 0.02–2.0 (m^{-1}) for μ_w as a function of the wavelength. Values of μ_w in the range of 0.68 ± 0.35 (m^{-1}) have been reported by Megard et al. (1979). Chlorophyll extinction coefficient is species-dependent. Values in the range of 0.2–31.4 ($\text{m}^2\text{g}^{-1}\text{Chla}$) with mean spectral value of 16.0 were reported by Bannister (1979, 1974) for μ_{ch} while Megard et al. (1979) reported values of 22 ± 5 ($\text{m}^2\text{g}^{-1}\text{Chla}$) for the photosynthetically active radiation.

MODEL GENERALIZATION

In order to apply the lake water temperature numerical model to lakes for which no site-specific calibration has been made, the model had to be generalized. This was accomplished by introducing functional relationships for the model coefficients that are valid for lakes on a regional rather than individual basis. A large Minnesota lake database was used to derive these general relationships.

Hypolimnetic Diffusivity Closure

Although the hypolimnion is isolated from the surface (epilimnetic) layer by the thermocline and its associated density gradient, strong and sporadic local mixing events have been observed in the hypolimnion (Jassby and Powell 1975; Imberger 1985; Imberger and Patterson 1989). Heat flux between water and lake sediments was found to be important in eddy diffusivity estimation for inland shallow (10-m maximum depth) lakes, representative of the north central United States (Hondzo et al. 1991). Hypolimnetic eddy diffusivity dependence on stratification strength as measured by stability frequency has been pointed out consistently (Colman and Armstrong 1987; Gargett 1984; Gargett and Holloway 1984; Hondzo et al. 1991; Quay et al. 1980). Stability frequency is related to hypolimnetic eddy diffusivity by:

$$K_z = \alpha(N^2)^{-\gamma} \quad \dots\dots\dots (12)$$

where stability frequency $N^2 = -(\partial\rho/\partial z)(g/\rho)$, in which ρ = density of water, and g = acceleration of gravity, γ is determined by the mode of turbulence production (narrow or broad band internal waves, local shear, etc.), and α is determined by the general level of turbulence. For most inland lakes, coefficient γ ranges from 0.4 to 0.6 (Ellis and Stefan 1991; Hondzo et al. 1991; Quay et al. 1980; Jassby and Powell 1975; Gerhard et al. 1990).

Hypolimnetic eddy diffusivity estimations in four northern Minnesota lakes follow (12) as shown in Fig. 1. K_z was estimated from temperature profiles (Hondzo et al. 1991) by a flux gradient technique. Dimensionless analysis (Ward 1977) suggests that lake surface area can provide horizontal scale for the vertical eddy diffusivity estimation. The vertical scale (lake depth) is implicitly built into the stability frequency. The α coefficient in (12) is plotted as a function of lake surface area in Fig. 2. A general relationship applicable to lakes on a regional scale was therefore summarized as:

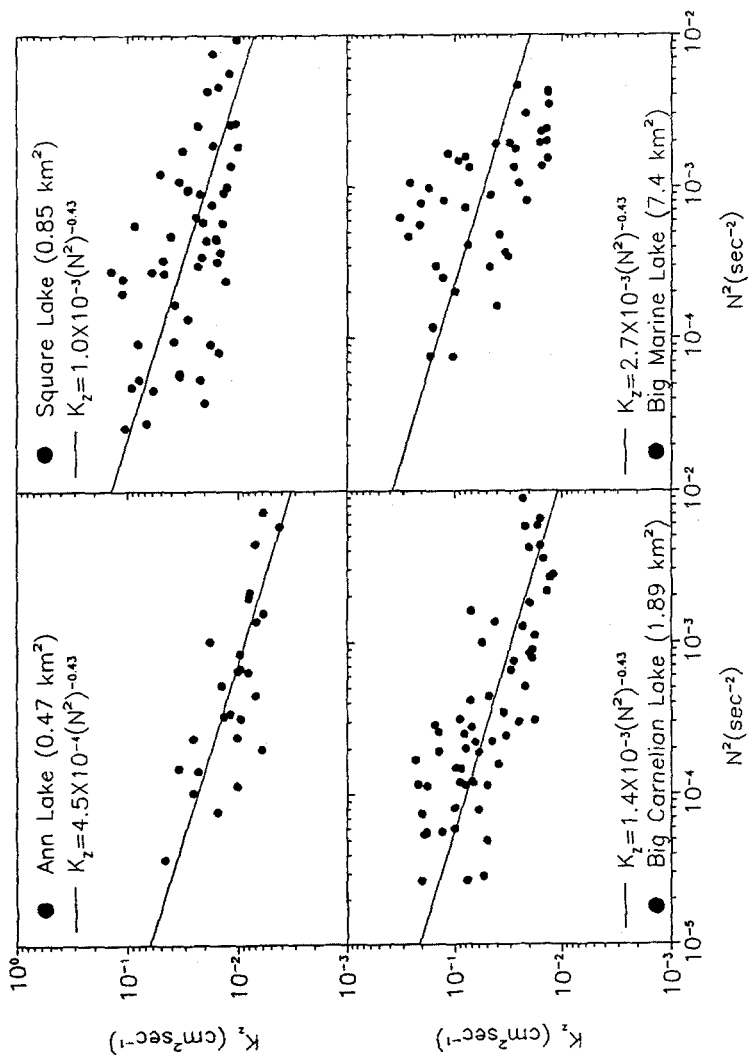


FIG. 1. Hypolimnetic Eddy Diffusivity Dependence on Lake Surface Area

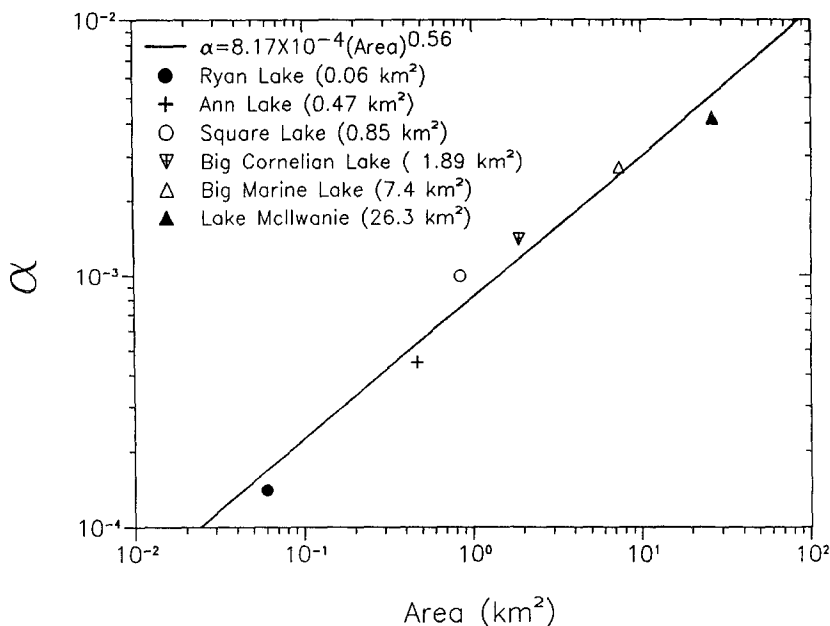


FIG. 2. Hypolimnetic Eddy Diffusivity Forcing Parameter (α) Dependence on Lake Surface Area

$$K_z = 8.17 \times 10^{-4} (A_s)^{0.56} (N^2)^{-0.43} \quad (13)$$

where A_s = lake surface area (km^2), N^2 is in sec^{-2} , and K_z is in $\text{cm}^2 \text{sec}^{-1}$.

Maximum vertical hypolimnetic eddy diffusivity, $K_{z\max}$, obtained from temperature profiles under weakly stratified conditions, which were defined as $N^2 = 7.0 \times 10^{-5} \text{ sec}^{-2}$ (Riley and Stefan 1987), was also correlated with lake surface area because turbulent mixing in nonstratified lakes depends strongly on kinetic wind energy supplied, which in turn depends on lake surface area. Maximum hypolimnetic eddy diffusivity versus lake surface area for eight different lakes is plotted in Fig. 3. Data are from Jassby and Powell (1975), Ward (1977), and Lewis (1983), and from this study.

Wind Sheltering Coefficient

The wind sheltering coefficient is a function of lake surface area (fetch). The turbulent kinetic energy computation [(10)] uses a wind speed taken from an off-site weather station at 10-m elevation and adjusts that wind speed for fetch over the lake in the direction of the wind. As wind speed typically increases with fetch, the calculated downstream wind speed is an estimate of the maximum wind speed on the lake surface. Typically fetch on a lake is reduced by wind sheltering on the upwind side of the lake where the wind makes a transition from a landbound turbulent velocity profile to the open water (Ford and Stefan 1980). Trees or buildings along the shoreline will shelter a larger portion of a small lake than a large one. The downwind maximum wind speed does not grow linearly with fetch. A maximum wind speed at the downwind end of a large lake will be more representative than for a small one. Biweekly temperature profile measurements in 10 lakes and throughout the summer season were used to optimize

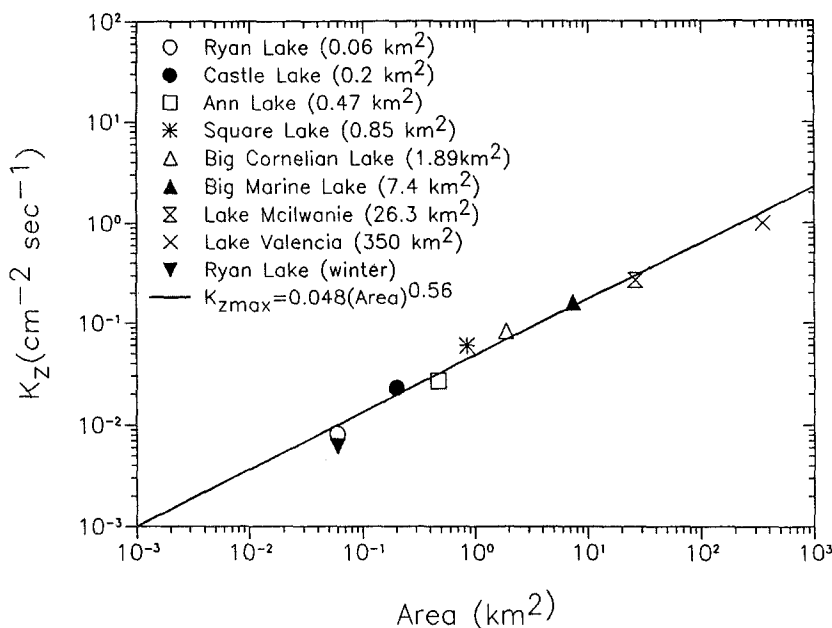


FIG. 3. Maximum Hypolimnetic Eddy Diffusivity (at $N^2 = 7.5 \cdot 10^{-5} \text{ sec}^{-2}$) Dependence on Lake Surface Area

the wind sheltering coefficients W_{str} against lake surface area (km^2) (Fig. 4). The empirical relationship is

$$W_{str} = 1.0 - \exp(-0.3 \times A_s) \dots \dots \dots (14)$$

The low values in Fig. 4 indicate that the modeling of wind mixing in small lakes depends very much more on a correct estimate of the amount of wind energy supplied. Because wind energy also has a physical relationship to lake eddy diffusivity a similarity between Figs. 4 and 3 is expected.

Wind Function Coefficient

The wind function coefficient (c) defined in (11) enters into the convective heat transfer relationships (8) and (9), and depends also on lake surface area (fetch) as was found by Harbeck (1962) and Sweers (1976), and summarized by Adams et al. (1990). Harbeck (1962) analyzed data from lakes of different sizes and pointed out that evaporation rates in small and large lakes might be the same. The fetch dependence is introduced to account for the wind speed increase with distance over the water. In this numerical model off-lake wind speeds measured at permanent weather stations are used, but they are adjusted for lake fetch (Ford and Stefan 1980). Nevertheless, some residual wind function coefficient dependence on lake fetch is shown in Table 2. A functional relationship was obtained by plotting the wind function coefficient from several previous numerical model simulations against lake surface area (Fig. 5). The estimated relationship is:

$$c = 24 + \ln(A_s) \dots \dots \dots (15)$$

where A_s is again lake surface area in km^2 . This relationship shows only a

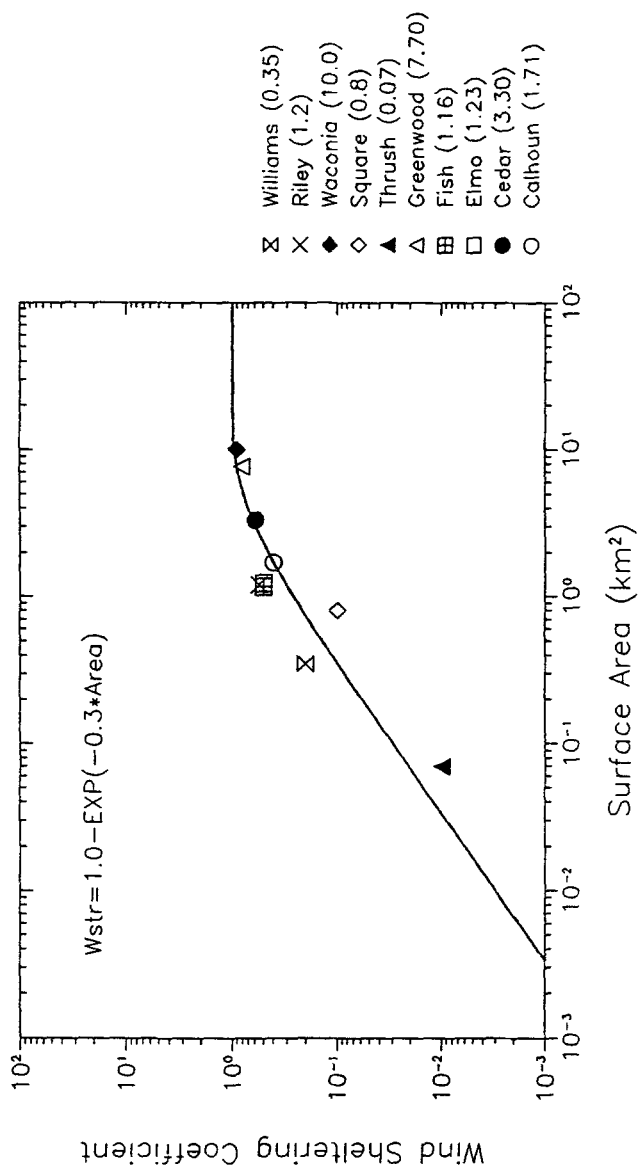


FIG. 4. Wind Sheltering Coefficient Dependence on Lake Surface Area

TABLE 2. Coefficients for Calibration of Water Temperature Model

Lake (1)	Year (2)	Maxi- mum depth	Sur- face area	Wind function coefficient	Wind shelter coefficient	Attenuation Coefficient		Chla (mg m ⁻³) (9)
		H_{max} (m) (3)	A_s (km ²) (4)	c (—) (5)	W_{str} (—) (6)	μ_w (m ⁻¹) (7)	μ_{chl} (m ² g ⁻¹ chla) (8)	
Calhoun	1971	24.0	1.71	24	0.40	0.65	8.65	4–37 ^a
Cedar	1984	4.70	3.30	24	0.60	0.65	8.65	6–130 ^b
Elmo	1988	41.8	1.23	26	0.50	0.65	8.65	3–8 ^c
Fish	1987	8.20	1.16	26	0.50	1.00	8.65	18–48 ^d
Square	1985	21.0	0.85	24	0.10	0.50	8.65	1–4 ^e
Waconia	1985	11.0	10.0	27	0.90	0.65	8.65	11–34 ^f
Greenwood	1986	34.0	7.70	29	0.80	0.65	8.65	1–3 ^d
Thrush	1986	14.0	0.07	24	0.01	0.65	8.65	2–4 ^e
Williams	1984	10.0	0.35	22	0.20	0.65	8.65	3–7 ^f

^aShapiro and Pfannkuch (1973) field data.^bOsgood (1984) field data.^cOsgood (1989) field data.^dHeiskarg and Wilson (1988) field data.^eWright et al. (1988) field data.^fWinter (1980) field data.

weak dependence of c on lake surface area A_s and can be viewed as a minor adjustment. This adjustment is necessary because the wind speed used in the heat transfer equations, (8) and (9), is at the downwind end of the lake and therefore an overestimate of the average wind speed over the lake surface. Because of the nonlinearity of wind speed with distance the overestimate is more severe for small lakes than for large lakes. Therefore the wind function coefficient has to be smaller for smaller lakes in order to compensate for the wind velocity overestimate. If wind speeds are measured on the lake (middle of the lake) and not off-lake, the situation is reversed. This reversed trend of wind function coefficient with lake surface area was found and reported by Harbeck (1962) and Sweers (1976), and summarized by Adams et al. (1990). All of these used on-lake wind measurements.

Attenuation Coefficients

The specific radiation attenuation coefficients for water and chlorophyll were replaced by the total attenuation coefficient. This was done following the principle of parsimony, i.e., the fewer coefficients in the model, the less uncertain the model estimate. In addition, uncertainty analysis showed that chlorophyll-a made a minor contribution to lake water temperature uncertainty. A relationship between total attenuation coefficient μ (m⁻¹) and Secchi depth z_{sd} (m) was obtained from measurements in 50 lakes in Minnesota (Osgood 1990) and is plotted in Fig. 6.

$$\mu = 1.84(z_{sd})^{-1} \dots \dots \dots (16)$$

The form of this relationship has been found to be valid in inland waters in general (Idso and Gilbert 1974) and in the ocean (Poole and Atkins 1929).

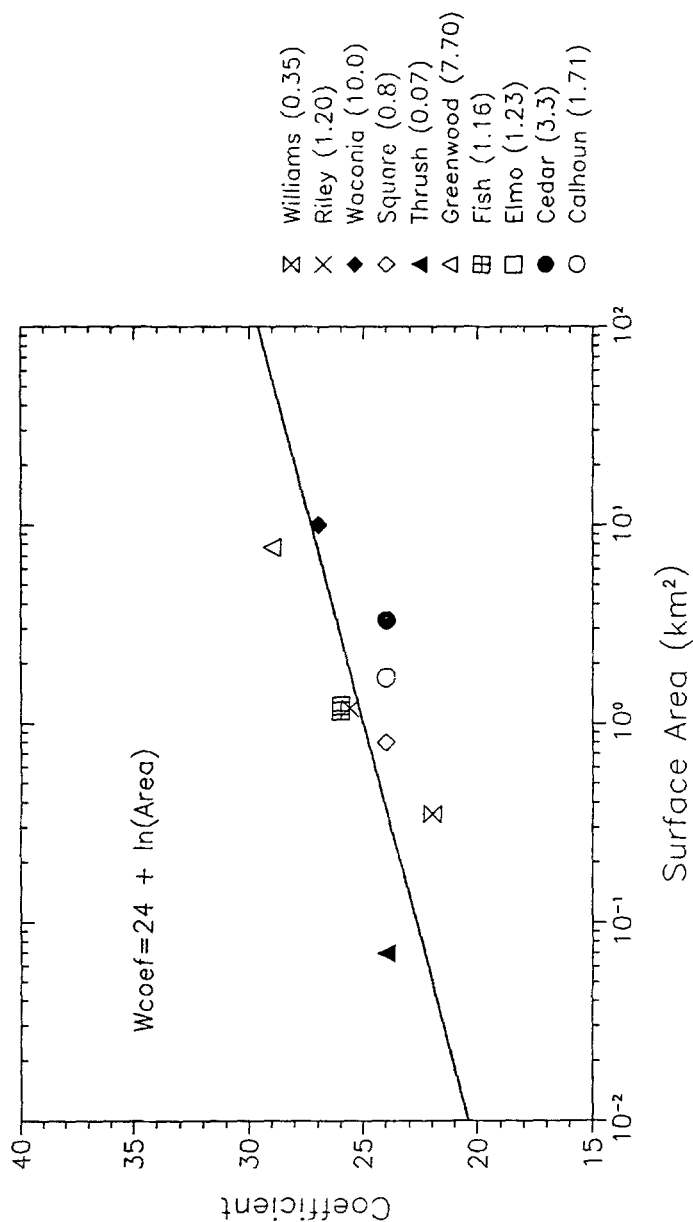


FIG. 5. Wind Function Coefficient Dependence on Lake Surface Area

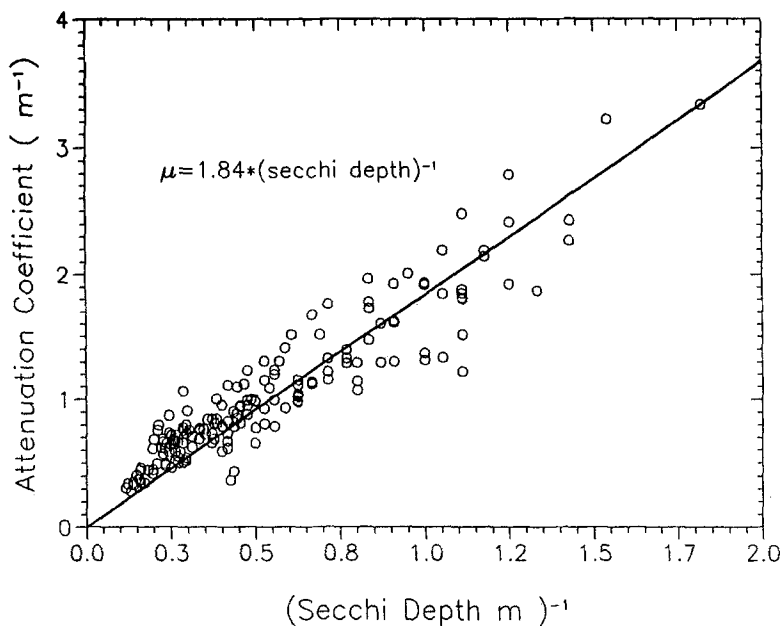


FIG. 6. Relationship between Total Attenuation Coefficient and Secchi Disk Depth

WATER TEMPERATURE MODEL VALIDATION AFTER GENERALIZATION OF HYPOLIMNETIC EDDY DIFFUSIVITY

The model was first modified by adding the hypolimnetic eddy diffusivity closure [(13)]. The number of calibration coefficients was thereby reduced from five to four. The remaining four are W_{str} , c , μ_w , and μ_{chl} . The modified numerical model then had to be validated with water temperature measurements in several selected lakes over a period of several years. Representative lakes in Minnesota were selected through an analysis of the state's extensive data bases. "Representative" meant a lake either having values of lake surface area, maximum depth, and secchi depth near the median as identified in a state report by the Minnesota Pollution Agency (Heiskary et al. 1988) or being near the far ends of the respective frequency distributions for ecoregions. Selected representative lakes with their position on the cumulative frequency distribution curves for northern and southern Minnesota are given in Fig. 7. Lakes covered the entire range of maximum depths (shallow-medium-deep), surface area (small-medium-large), and trophic status (eutrophic-mesotrophic-oligotrophic).

To validate the model, numerical simulations were started with isothermal conditions (4°C) on March 1 and continued in daily time steps until November 30. Ice goes out of Minnesota lakes sometime between the end of March and beginning of May. Dates of spring overturn vary with latitude and year. To allow for these variable conditions, a 4°C isothermal condition was imposed until simulated daily water temperatures began to rise above 4°C. This method permitted the model to find its own date of spring overturn (4°C) and the simulated summer heating cycle started from that date (Hondzo and Stefan 1991).

Daily meteorological data files were assembled from Minneapolis/St. Paul,

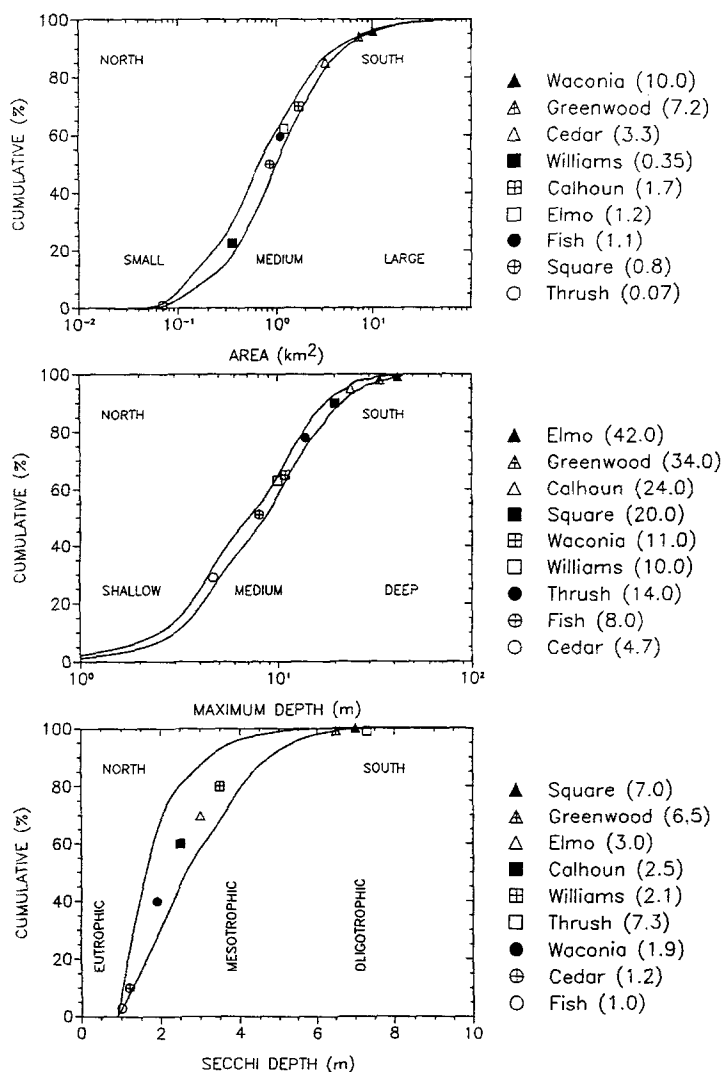


FIG. 7. Cumulative Distributions (%) of Lake Parameters in Minnesota Lakes; Selected Lakes for Model Validation are Shown by Symbols

and Duluth, for southern and northern Minnesota, respectively. These two stations were selected because there are no other stations in the state that provide all required meteorological variables. The two stations account for spatial variability in meteorological forcing between southern and northern Minnesota, respectively, and are as close to the main lake areas as stations in the neighboring states. Distances between the stations and simulated lakes were as large as 200 km, but the flat and open plains topography justifies to a reasonable extent the regional transfer of weather data.

A quantitative measure of the success of the simulations for nine rep-

representative lakes is given in Table 3. Different gauges of the simulation success are defined as: (1) Volume weighted temperature averages

$$\hat{T}_s = \frac{\sum_{i=1}^p V_i T_{si}}{\sum_{i=1}^p V_i} \dots\dots\dots (17a)$$

$$\hat{T}_m = \frac{\sum_{i=1}^p V_i T_{mi}}{\sum_{i=1}^p V_i} \dots\dots\dots (17b)$$

(2) temperature root mean square errors

$$E_1 = \left[\frac{\sum_{i=1}^p (T_{si} - T_{mi})^2}{p} \right]^{0.5} \dots\dots\dots (18a)$$

$$E_2 = \left[\frac{\sum_{i=1}^p V_i (T_{si} - T_{mi})^2}{\sum_{i=1}^p V_i} \right]^{0.5} \dots\dots\dots (18b)$$

and (3) r^2 , i.e., that portion of the temperature measurements explained by the simulations (Riley and Stefan 1987). In the aforementioned equations subscripts i , s , and m refer to the counting index, simulated, and measured temperature respectively. V_i = the water volume of a layer in the stratified lake. The aforementioned parameters are estimated by summing over lake

TABLE 3. Quantitative Measure of Success of Simulations

Lake (1)	Year (2)	Num- ber of field data (3)	\hat{T}_m (°C) (4)	Validated Model				Differences (Regional- Validated Model)			
				\hat{T}_s (°C) (5)	E_1 (°C) (6)	E_2 (°C) (7)	r^2 (8)	$\Delta \hat{T}_s$ (°C) (9)	ΔE_1 (°C) (10)	ΔE_2 (°C) (11)	Δr^2 (%) (12)
Calhoun	1971	136	14.37	14.52	0.86	0.79	0.97	-0.08	0.16	0.10	-1
Cedar	1984	20	20.64	20.86	0.94	0.99	0.93	-0.18	0.13	0.16	-2
Elmo	1988	214	13.94	14.09	1.77	1.80	0.92	0.22	0.06	0.13	-2
Fish	1987	32	24.40	24.13	0.80	0.82	0.90	-0.23	0.07	0.07	-1
Square	1985	136	14.37	14.52	0.86	0.79	0.97	0.38	0.38	0.24	-2
Waconia	1985	43	20.14	20.12	0.78	0.73	0.92	-0.03	-0.10	-0.05	2
Greenwood	1986	46	11.80	11.97	0.89	0.79	0.93	0.64	0.35	0.20	-1
Thrush	1986	114	11.97	11.91	0.90	0.91	0.96	0.63	0.05	0.06	-1
Williams	1984	110	17.26	16.37	1.08	1.07	0.97	0.20	0.18	0.18	-1
Average	—	95	16.54	16.49	0.97	0.96	0.94	0.17	0.14	0.12	-1

Note: \hat{T}_m = measured volume weighted average temperature; \hat{T}_s = simulated volume weighted average temperature; E_1 = temperature root mean square error; E_2 = volume weighted temperature root mean square error; and r^2 = portion of measured water temperature variability explained by simulations.

depths. Overall seasonal average parameters are reported in Table 3 (validated model). One example of simulated and measured vertical lake water temperature profiles is given in Fig. 8. Other examples can be found in a report by Hondzo and Stefan (1992). The model simulates onset of stratification, mixed layer depth, and water temperatures well.

Volume weighted and unweighted root mean square error was less than 1°C for all lakes except the deepest (Lake Elmo has a maximum depth of 40 m). This is mostly due to small differences in predicted thermocline depth for the deepest simulated lake. Differences between the two estimated root mean square errors (E_1 and E_2) indicate the vertical position of the maximum simulation error. If E_2 is greater than E_1 , then the differences between measured and simulated lake water temperatures are greater in the surface water layers because E_2 values are volume weighted and E_1 values are not. The average root mean square error for all lakes was 1°C , and 94% ($r^2 = 0.94$) of water temperature measurements variability was explained by the numerical model.

Model coefficients used in the simulations are given in Table 2. These

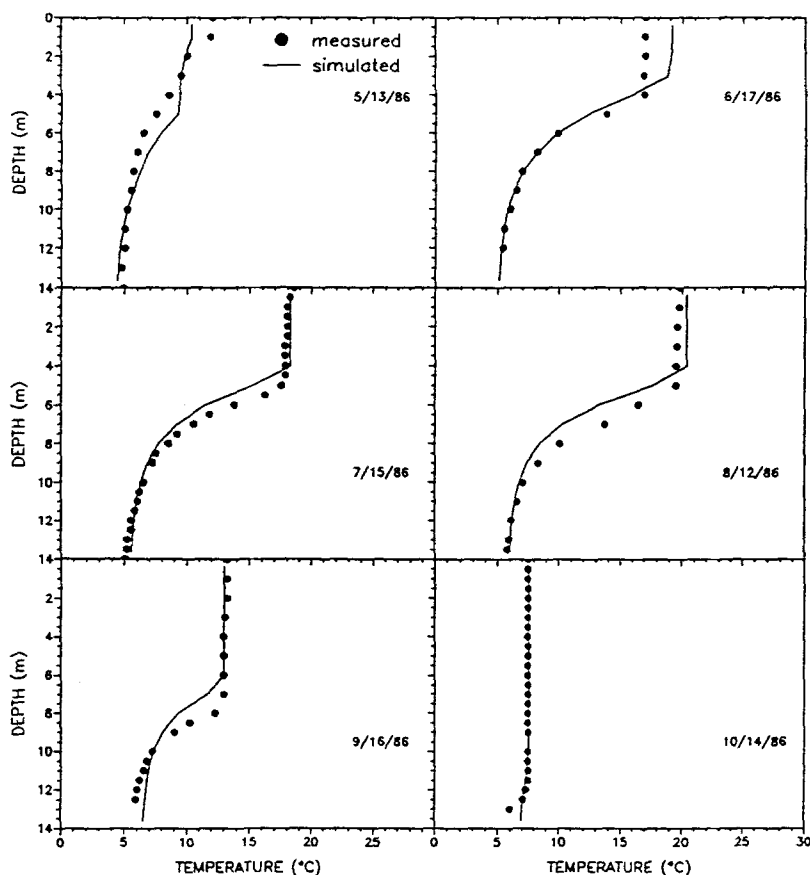


FIG. 8. Thrush Lake Water Temperature Profiles

coefficients give minimum values of root mean square error, and highest value of r^2 between measurements and simulated lake water temperatures.

In the following sections the modified model with the hypolimnetic eddy diffusivity closure as described in this section will be referred to as the validated model.

NUMERICAL UNCERTAINTY OF MODEL AFTER HYPOLIMNETIC CLOSURE

Uncertainty in the lake water temperature simulations was considered in terms of all model coefficients except maximum hypolimnetic eddy diffusivity as specified in Table 1. To first-order the uncertainty in lake water temperature depends on the uncertainty in the model coefficients, and on the sensitivity of the lake water temperatures to changes in the coefficients:

$$\begin{aligned}
 P_T &= E[(T - \hat{T})(T - \hat{T})^T] \\
 &\approx E \left\{ \left[T(\hat{u}) + \frac{\partial T}{\partial u}(u - \hat{u}) - \hat{T} \right] \left[T(\hat{u}) + \frac{\partial T}{\partial u}(u - \hat{u}) - \hat{T} \right]^T \right\} \\
 &= E \left\{ \left[\frac{\partial T}{\partial u}(u - \hat{u}) \right] \left[\frac{\partial T}{\partial u}(u - \hat{u}) \right]^T \right\} = \frac{\partial T}{\partial u} E[(u - \hat{u})(u - \hat{u})^T] \frac{\partial T^T}{\partial u} \\
 &= \frac{\partial T}{\partial u} P_u \frac{\partial T^T}{\partial u} \dots \dots \dots (19)
 \end{aligned}$$

where P_T = the $(m \times m)$ covariance matrix of the simulated lake water temperatures, m = the total number of discretized lake control volumes, $E\{\cdot\}$ = the mathematical expectation, \hat{T} = the mean lake water temperature, tr = the transpose, u = the vector of the n coefficients, P_u = the $(n \times n)$ covariance matrix of system coefficients, and $\partial T/\partial u$ = the $(m \times n)$ sensitivity matrix of partial derivatives of the lake water temperatures with respect to the coefficients. The sensitivity matrix is estimated using the influence coefficient method (Willis and Yeh 1987).

Data for the system coefficients covariance matrix are given in Table 4. These values were chosen to be in the range of theoretical and simulated values (Table 1), and to have coefficients of variation (standard deviation/mean) equal to 0.3. This value is chosen because first-order uncertainty analysis could be questionable when the coefficient of variation of a nonlinear function increases above 0.3.

Three lakes are selected for the lake water temperature uncertainty estimation. Lake Calhoun is a eutrophic, deep (24-m maximum depth) lake,

TABLE 4. Coefficients for Uncertainty Analysis

Coefficient (1)	Lake Calhoun		Williams Lake		Cedar Lake	
	Mean (2)	Standard deviation (3)	Mean (4)	Standard deviation (5)	Mean (6)	Standard deviation (7)
μ_w (m^{-1})	0.65	0.20	0.65	0.20	0.65	0.20
μ_{ch} ($m^2 g^{-1} Chla$)	8.65	2.65	8.65	2.65	8.65	2.65
W_{str}	0.60	0.18	0.20	0.06	0.60	0.18
c	24.0	7.20	20.0	6.00	24.0	7.20

Williams Lake is oligotrophic, and has maximum depth close to the median depth of 3,002 lakes in Minnesota, and Cedar Lake is a highly eutrophic shallow (4.7-m maximum depth) lake.

Standard deviations of smoothed simulated epilimnion and volume-weighted average hypolimnion temperatures are given for one sample lake in Fig. 9. Although high variability in model coefficients was imposed, maximum standard deviation in epilimnion temperatures was less than 1°C , and less than 1.5°C for the hypolimnion temperatures. Epilimnion temperatures are most sensitive to the wind function coefficient for all three lakes. In the shallow and well-mixed Cedar Lake the wind function coefficient is the only one that significantly contributes to lake water temperature uncertainty. The lowest variability of lake water temperature uncertainty is associated with radiation attenuation by phytoplankton (Chlorophyll-a). Variability in water attenuation and wind sheltering contribute less to uncertainty in epilimnion lake water temperatures than the wind function coefficient. Volume weighted hypolimnion temperatures displayed higher uncertainty than epilimnion temperatures. For Williams Lake and Lake Calhoun, all three coefficients, i.e., water attenuation, wind sheltering, and wind function coefficient significantly contributed to the lake water temperature uncertainty.

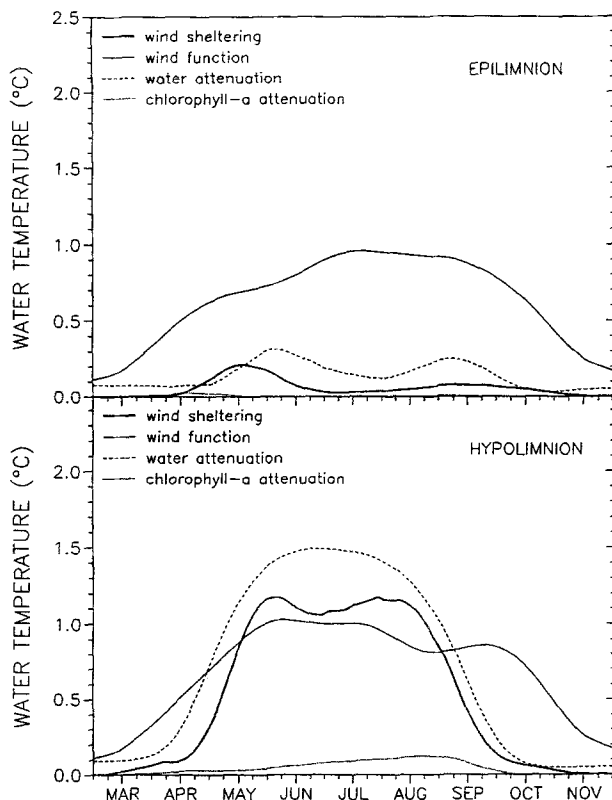


FIG. 9. Standard Deviations of Estimated Lake Water Temperature Uncertainties—Williams Lake

Schindler (1988) pointed out that in oligotrophic lakes dissolved organic carbon is one of the major light attenuating factors.

ACCURACY OF REGIONAL MODEL AFTER IMPLEMENTATION OF ALL CHANGES

The number of calibration coefficients was reduced from five to zero. Functional relationships substituted in the model are given in (13), (14), (15), and (16). The model was compared with water temperature measurements in nine selected representative lakes. Simulations started with isothermal conditions (4°C) on March 1 and progressed in daily time steps until November 30. Quantitative measure of the success of the simulations and differences between the regional model and the validated model are given in Table 2. The average weighted and unweighted root mean square error was 1.1°C (16.5°C average measured lake water temperature). Ninety three percent of measured lake water temperature variability was explained by the numerical simulations ($r^2 = 0.93$). The regional model has an average 0.15°C higher temperature root mean square error.

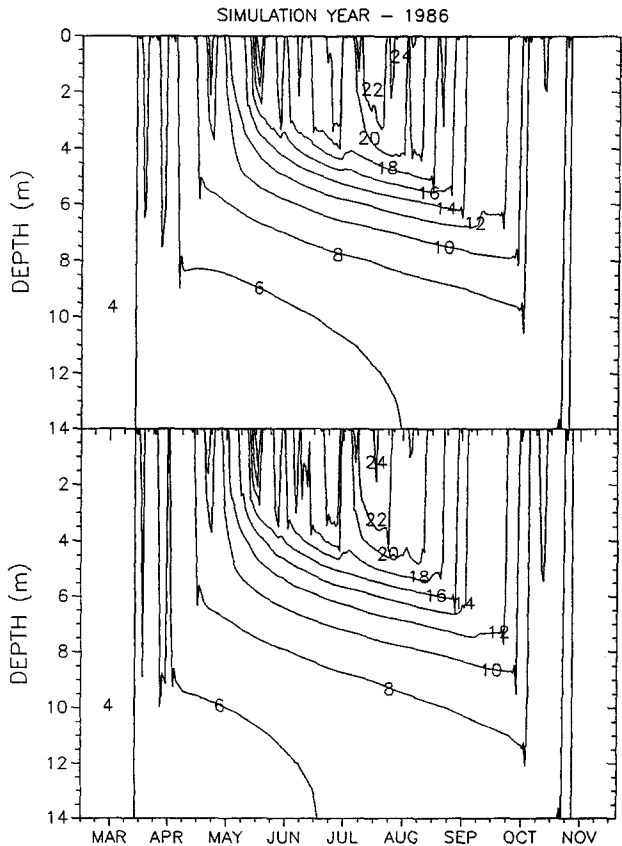


FIG. 10. Simulated Temperature (Isotherm) Structure in Thrush Lake; Top Shows Results from Validated Model and Bottom Shows Results from Regional Model

One example of the daily simulated isotherms for the regional and the validated model is given in Fig. 10. Both models simulate onset of stratification, mixed layer depth, and water temperatures in a virtually identical way.

CONCLUSIONS

A lake-specific water temperature model was generalized for the application to a wide range of lake classes and meteorological conditions. Functional relationships that apply to lakes on a region rather than to individual lake were developed.

Hypolimnetic eddy diffusivity was estimated as a function of lake surface area and stability frequency. Eq. (13) extends Ward's (1977) analysis to a wider range of lake geometries. Although the proposed relationship is a significant simplification of the turbulent diffusion processes taking place in the hypolimnion, it was found to be useful in the seasonal lake water temperature modeling.

Total attenuation coefficient was estimated as a function of Secchi depth (Fig. 6). Secchi depth is chosen because of its simplicity of measurement. It is commonly available.

Wind sheltering and wind function coefficients increase with surface area (fetch) of the lake (Figs. 4 and 5). The wind function coefficient increase is very likely an additional adjustment of the wind velocity coming from land over the lake surface.

Uncertainty analysis revealed moderate sensitivity of simulated lake water temperatures to the individual model coefficients. This could be due to the high thermal inertia of the water especially for the seasonal lake water temperature modeling. Nevertheless epilimnion temperatures showed 1°C standard deviations due to the wind function coefficient variability. Water attenuation, wind function, and wind sheltering coefficients equally contribute to the hypolimnetic temperatures variability in an oligotrophic lake.

The proposed model has practical application in late water temperature modeling, especially in lakes where measurements are not available. The regional model simulates onset of stratification, mixed layer depth, and water temperatures well. Average temperature mean square error was 1.1°C, and 93% of measured lake water temperature variability was explained by the numerical simulations over a wide range of lake classes and trophic levels.

ACKNOWLEDGMENTS

Material presented in this paper was developed with partial support from the USEPA/ERLD, John G. Eaton project officer. We would especially like to thank several researchers who provided lake data: Tom Winter, U.S. Geological Survey, Williams Lake; Dick Osgood, Metropolitan Council, Metropolitan area lakes; David Wright, Minnesota Department of Natural Resources, Thrush Lake; and members of the Minnesota Pollution Control Agency, Greenwood Lake.

APPENDIX I. REFERENCES

- Adams, E. E., Cosler, D. J., and Helfrich, K. R. (1990). "Evaporation from heated water bodies: Predicting combined forced plus free convection." *Water Resour. Res.*, 26(3), 425–435.

- Aldama, A. A., Harleman, D. R. F., and Adams, E. E. (1989). "Hypolimnetic mixing in a weakly stratified lake." *Water Resour. Res.*, 25(5), 1014–1024.
- Bannister, T. T. (1974). "Production equations in terms of chlorophyll concentration, quantum yield, and upper limit to production." *Limnology and Oceanography*, 19(1), 1–12.
- Bannister, T. T. (1979). "Quantitative description of steady state, nutrient-saturated algal growth, including adaptation." *Limnology and Oceanography*, 24(1), 76–96.
- Colman, J. A., and Armstrong, D. E. (1987). "Vertical eddy diffusivity determined with ^{222}Rn in the benthic boundary layer of ice-covered lakes." *Limnology and Oceanography*, 32(3), 577–590.
- Dake, J. M. K. (1972). "Evaporative cooling of a body of water." *Water Resour. Res.*, 8(4), 1087–1091.
- Dake, J. M. K., and Harleman, D. R. F. (1969). "Thermal stratification in lakes: Analytical and laboratory studies." *Water Resour. Res.*, 5(2), 404–495.
- Dhamotharan, S. (1979). "A mathematical model for temperature and turbidity stratification dynamics in shallow reservoirs," PhD thesis, University of Minnesota, 319.
- Ellis, C., and Stefan, H. G. (1991). "Water temperature dynamics and heat transfer beneath the ice cover of a lake." *Limnology and Oceanography*, 36(2), 324–335.
- Ford, D. E. (1976). "Water temperature dynamics of dimictic lakes: Analysis and prediction using integral energy concepts," PhD thesis, University of Minnesota, 432.
- Ford, D. E., and Stefan, H. G. (1980). "Thermal predictions using integral energy model." *J. Hydr. Div.*, ASCE, 106(1), 39–55.
- Gargett, A. E. (1984). "Vertical eddy diffusivity in the ocean interior." *J. Marine Res.*, 42(2), 359–393.
- Gargett, A. E., and Holloway, G. (1984). "Dissipation and diffusion by internal wave breaking." *J. Marine Res.*, 42(1), 15–27.
- Gerhard, H., Imberger, J., and Schimmele, M. (1990). "Vertical mixing in Ueberlinger See, western part of Lake Constance." *Aquatic Sci.*, 53(3), 256–268.
- Harbeck, G. E., Jr. (1962). "A practical field technique for measuring reservoir evaporation utilizing mass-transfer theory." *Prof. Paper 272E*, U.S. Geological Survey, 101–105.
- Harleman, D. R. F. (1982). "Hydrothermal analysis of lakes and reservoirs." *J. Hydr. Div.*, ASCE, 108, 302–325.
- Heiskary, S. A., and Wilson, C. B. (1988). *Minnesota lake water quality assessment report*, Minnesota Pollution Control Agency, St. Paul, Minn., 49.
- Henderson-Sellers, B., and Davies, A. M. (1989). "Thermal stratification modeling for oceans and lakes." *Annual Review of Numerical Fluid Mechanics and Heat Transfer*, Vol. 2, C. L. Tien and T. H. Chawla, eds., Hemisphere, New York, N.Y., 85–156.
- Hondzo, M., Ellis, C., and Stefan, H. G. (1991). "Vertical diffusion in small stratified lake: Data and error analysis." *J. Hydraul. Engrg.*, ASCE, 117(10), 1352–1369.
- Hondzo, M., and Stefan, H. G. (1991). "Three case studies of lake temperature and stratification response to warmer climate." *Water Resour. Res.*, 27(8), 1837–1846.
- Hondzo, M., and Stefan, H. G. (1992). "Water temperature characteristics of lakes subjected to climate change." *Project Report No. 329*, St. Anthony Falls Hydr. Lab., Univ. of Minnesota, Minneapolis, Minn., 185.
- Idso, S. B., and Gilbert, R. G. (1974). "On the universality of the Poole and Atkins Secchi disk-light extinction equation." *J. Appl. Ecology*, 11, 399–401.
- Idso, S. B., and Jackson, R. D. (1969). "Thermal radiation from the atmosphere." *J. Geophysical Res.*, 74(23), 5397–5403.
- Imberger, J. (1985). "The diurnal mixed layer." *Limnology and Oceanography*, 30(4), 737–770.
- Imberger, J., and Patterson, J. C. (1989). "Physical limnology." *Advances in applied mechanics*, J. W. Hutchinson and T. Y. Wu, eds., Vol. 27, Academic Press, San Diego, Calif., 303–475.
- Jassby, A., and Powell, T. (1975). "Vertical patterns of eddy diffusion during strat-

- ification in Castle lake, California." *Limnology and Oceanography*, 20(4), 530–543.
- Lewis, W. M. Jr. (1983). "Temperature, heat, and mixing in Lake Valencia, Venezuela." *Limnology and Oceanography*, 28(2), 273–286.
- Megard, R. O., Combs, W. S. Jr., Smith, P. D., and Knoll, A. S. (1979). "Attenuation of light and daily integral rates of photosynthesis attained by planktonic algae." *Limnology and Oceanography*, 24(6), 1038–1050.
- McCormick, M. J. (1990). "Potential changes in thermal structure and cycle of Lake Michigan due to global warming." *Trans. American Fisheries Society*, 119(2), 183–194.
- Osgood, R. A. (1984). "A 1984 study of the water quality of 43 metropolitan area lakes." *Publication No. 10-84-172*, Metropolitan Council, St. Paul, Minn., 40.
- Osgood, R. A. (1989). "An evaluation of the effects of watershed treatment systems on summertime phosphorus concentration in metropolitan area lakes." *Publication No. 590-89-062*, Metropolitan Council, St. Paul, Minn., 85.
- Poole, H. H., and Atkins, W. R. G. (1929). "Photo-electric measurements of submarine illumination throughout the year." *J. Marine Biology Association of United Kingdom*, 16, 297–324.
- Quay, P. D., Broecker, W. S., Hesslein, R. H., and Schindler, D. W. (1980). "Vertical diffusion rates determined by tritium tracer experiments in the thermocline and hypolimnion of two lakes." *Limnology and Oceanography*, 25(2), 201–218.
- Riley, M. J., and Stefan, H. G. (1987). "Dynamic lake water quality simulation model 'Minlake.'" *Report No. 263*, St. Anthony Falls Hydraulic Laboratory, University of Minnesota, Minneapolis, Minn., 140.
- Schertzer, W. M., and Sawchuk, A. M. (1990). "Thermal structure of the lower Great Lakes in a warm year: Implications for the occurrence of hypolimnion anoxia." *Trans. Amer. Fisheries Society*, 119(2), 195–209.
- Schindler, D. W., Beaty, K. G., Fee, E. J., Cruikshank, D. R., DeBruyn, E. R., Findley, D. L., Londsey, G. A., Sherer, J. A., Stainton, M., and Turner, M. A. (1990). "Effects of climatic warming on lakes of the Central Boreal Forest." *Science*, 250(16), 967–970.
- Shapiro, J., and Flannkuch, H. (1973). *The Minneapolis chain of lakes: A study of urban drainage and its effects 1971–1973*, Limnological Research Center, University of Minnesota, Minneapolis, Minn.
- Smith, C. R., and Baker, K. S. (1981). "Optical properties of the clearest natural waters." *Appl. Optics*, 20(2), 177–184.
- Stefan, H. G., Cardoni, J. J., Schiebe, F. R., and Cooper, C. M. (1983). "Model of light penetration in a turbid lake." *Water Resour. Res.*, 19(1), 109–120.
- Stefan, H. G., Dhamotharan, S., and Schiebe, F. R. (1982). "Temperature/sediment model for a shallow lake." *J. Envir. Engrg. Div.*, ASCE, 108(4), 750–765.
- Stefan, H. G., and Ford, D. E. (1975). "Temperature dynamics in dimictic lakes." *J. Hydr. Div.*, ASCE, 101(1), 97–114.
- Stefan, H. G., Gulliver, J., Hahn, M. G., and Fu, A. Y. (1980a). "Water temperature dynamics in experimental field channels: Analysis and modeling." *Report No. 193*, St. Anthony Falls Hydraulic Laboratory, University of Minnesota, Minneapolis, Minn.
- Stefan, H. G., Hanson, M. J., Ford, D. E., and Dhamotharan, S. (1980b). "Stratification and water quality predictions in shallow lakes and reservoirs." *Proc. Second Intl. Symp. on Stratified Flows*, International Association for Hydraulic Research, 1033–1043.
- Sweers, H. E. (1976). "A nomogram to estimate the heat-exchange coefficient at the air-water interface as a function of wind speed and temperature; a critical survey of some literature." *J. Hydrol.*, 30, 375–401.
- Ward, P. R. B. (1977). "Diffusion in lake hypolimnia." *Proc. 17th Congress Int. Association for Hydraulic Research*, International Association for Hydraulic Research, 103–110.
- Willis, R., and Yeh, W.W-G. (1987). *Groundwater systems planning and management*. Prentice-Hall, Englewood Cliffs, N.J., 415.

- Wright, D., Lawrenz, R., Popp, W., and Danks, M. (1988). "Acid precipitation mitigation program." *Progress Report Thrush Lake Minnesota*, Minnesota Dept. of Natural Resour. Div. of Fish and Wildlife Ecological Services Section, Kearneysville, W.V., 177.
- Wu, J. (1969). "Wind stress and surface roughness at air-sea interface." *J. Geophysical Res.*, 74(2), 444-455.

APPENDIX II. NOTATION

The following symbols are used in this paper:

- A = horizontal area of lake;
 A_s = lake surface area;
 C_d = momentum coefficient;
 C_l = vapour transfer coefficient;
 C_s = heat transfer coefficient;
 c = wind function coefficient;
 c_p = specific heat of water;
 $E\{\cdot\}$ = mathematical expectation;
 E_1 = temperature root mean square error;
 E_2 = volume weighted temperature root mean square error;
 $f(\cdot)$ = function of;
 H_a = atmospheric long wave radiation;
 H_{br} = back radiation;
 H_c = conductive loss;
 H_e = evaporative loss;
 H_n = net heat input at water surface;
 H_{sn} = net solar (short wave) radiation;
 K_{zmax} = maximum hypolimnetic eddy diffusivity;
 K_z = hypolimnetic eddy diffusivity;
 L_v = latent heat of vaporization;
 m = total number of lake control volumes;
 N^2 = stability frequency;
 P = precipitation;
 P_T = covariance matrix;
 p = total number of lake water temperature measurements;
 q' = specific humidity fluctuation;
 q_* = specific humidity scale;
 q_a = specific humidity above water surface;
 q_s = specific humidity at saturation pressure at water surface;
 r = reflection coefficient;
 T = water temperature;
 T_a = air temperature;
 T_d = dew point temperature;
 T_s = surface water temperature;
 \hat{T}_s = simulated volume weighted lake water temperature;
 \hat{T}_m = measured volume weighted lake water temperature;
 t = time;
 tr = transpose;
 U_a = wind speed;
 u = vector of coefficients;
 u' = turbulent fluctuation of velocity;

- u_* = velocity scale;
 V_i = lake volume between two layers;
 W_{str} = wind sheltering coefficient;
 w' = turbulent fluctuation of velocity;
 z = downward coordinate starting at lake surface;
 β = surface absorption coefficient;
 ε_a = atmospheric emissivity;
 ρ_a = density of air;
 ρ_w = density of water;
 τ = surface wind stress;
 θ' = turbulent fluctuation of temperature;
 θ_* = temperature scale;
 μ = total extinction coefficient;
 μ_{ch} = extinction coefficient due to phytoplankton (chlorophyll);
 μ_{ss} = extinction coefficient due to suspended sediment; and
 μ_w = extinction coefficient in water.

Subscripts

- i = counting index;
 mi = measured lake water temperature.
 si = simulated lake water temperature.